Molecular Dynamics Simulation of Bulk Atactic Polystyrene in the Vicinity of T_g

Alexey V. Lyulin* and M. A. J. Michels

Department of Applied Physics and Dutch Polymer Institute, Technische Universiteit Eindhoven, P.O. Box 513, 5600 MB Eindhoven, The Netherlands

Received July 24, 2001; Revised Manuscript Received November 12, 2001

ABSTRACT: Molecular dynamics (MD) simulations of bulk atactic polystyrene have been performed for chains up to 320 monomer units in a temperature range from 100 to 600 K and in a broad pressure range from 0.1 to 1000 MPa. The MD-determined specific volume vs temperature curves are in a good agreement with experimental PVT data at different values of applied pressure, but the measured glass-transition temperature, T_g, is displaced to somewhat higher temperature than the longer time experimental value. Local translational mobility has been investigated by measuring the mean-square translational displacements of monomers as a function of time. The long-time asymptotic slope of these dependencies is close to 0.6 at $T > T_g$, showing diffusive behavior. The cage effect, when local translational motions are essentially frozen in the glassy state, has been studied. The characteristic time of cage release does not depend on molecular weight, but the duration of the crossover to the diffusive regime increases almost linearly with increasing chain molecular weight, for both the backbone monomers and phenyl side groups.

1. Introduction

Our capability of understanding the structural and dynamic behavior of materials at high pressures and temperatures has in recent years been enhanced by the use of the molecular dynamics (MD) computer simulation methods. MD simulations are numerical solutions to classical Newtonian equations of motion for a set of particles interacting with the help of some interatomic potentials. MD simulations allow one to investigate the dynamics of a polymer system in microscopic detail, covering the rather wide time interval from femto- to nanoseconds and are widely used for the simulation of many different polymers, including important amorphous plastics such as, for example, polystyrene (PS). Polystyrene is an inexpensive and hard plastic, and probably only polyethylene and polypropylene are more common in our everyday life. At room temperature PS is in the glassy state, which is why the investigation of its dynamical properties and their connection to the glass-transition temperature, T_g, is rather important.

In the glassy state, when the temperature is lower than T_g , polymer coils are in general immobile. The obvious consequence of this immobility is the fact that the future rearrangement of the polymer structure upon cooling is highly restricted. This phenomenon is manifested, for example, through the changes of slope in specific volume vs temperature curves in the vicinity of T_g. Such changes in the temperature dependence of different properties can be observed in thermodynamic phase transitions, but the main difference between a phase and a glass transition is that the position of the latter depends on the cooling rate. In contrast to phase transitions, the glass transition is a relaxational kinetic process, not a thermodynamic one.

Polymer viscoelastic properties in the glassy state should be mainly influenced by local segmental motions. These motions are frequently explained by the redistribution of side groups (e.g., phenyl groups in PS), but the mechanism of this mobility remains unclear. Molecular dynamics gives a nice chance to investigate the local mobilities of the main chain and side groups independently.

The glass transition in polymer melts has been studied in great detail with Monte Carlo simulations using the bond fluctuation model.[1,2] The obvious drawbacks of these simulations are the complete neglect of local motions on the scale smaller than a lattice size. Constant-volume (NVT) and constant-pressure (NPT) molecular dynamics simulations of a dense model polymer liquid of 95 polymer chains with 10 monomers each have been performed by Bennemann et al.[3] They used a coarse-grained bead−spring model derived from the one suggested by Kremer and Grest[4] and took into account the attractive part of the Lennard-Jones potential. The main attention was paid to the investigation of the temperature dependence of the largest relaxation time in the melt (so-called α-relaxation) and, more precisely, the mean-square translational displacements of the inner monomers in the chain

$$g(t) = \langle [\mathbf{r}_i(t) - \mathbf{r}_i(0)]^2 \rangle \qquad (1)$$

where $\mathbf{r}_i$ is the radius vector of the ith bead. For short times one observes a ballistic regime which is followed by a subdiffusive regime and finally a free diffusion regime. In the vicinity of T_g the ballistic regime is followed by a plateaulike regime which precedes the subdiffusive one. The characteristic time of the onset of this subdiffusive regime describes the time scale at which a particle escapes from the cage formed by its neighbors. It was established that in this regime $g(t) \sim t^{\alpha}$ where $\alpha = 0.62 \pm 0.02$ for the monomer in the middle of the chain. Close values of $\alpha = 0.63$ and $\alpha = 0.553 \pm 0.026$ were also obtained by Bennemann et al.[5] and by Yip, Sylvester, and Argon,[6] respectively. The difference from the Rouse prediction $\alpha = 0.5$ was attributed to the shortness of the chains leading to an early crossover from the Rouse mode regime to the long-time free-diffusion limit. Detailed analysis of the dynamical

* To whom correspondence should be addressed. E-mail: a.v.lyulin@tue.nl.

10.1021/ma011318u CCC: $22.00
Published on Web 01/12/2002

properties of glass-forming polymers using molecular dynamics simulation was also performed by van Zon and de Leeuw[7] in attempts to study the predictions of mode-coupling theory.[8−10]

Structural and some dynamical properties of bulk atactic polystyrene have been simulated in a series of papers.[11−13] Rapold, Suter, and Theodorou[11] used detailed static atomistic simulations of glassy PS generated initially by a Monte Carlo procedure and equilibrated further by energy minimization. The results of these static simulations show that the frequency distribution of the phenyl ring motions covers many orders of magnitude: from rare 180° "ring flips" to gigahertz ring oscillations. In a series of papers[13] MD simulation of amorphous atactic PS has been performed using united-atom and all- atom models, in both of which the bond lengths were held fixed and the phenyl side groups were represented by rigid, planar hexagons. It was shown that the simulation results for the united-atom model successfully reproduce experimental data on X-ray scattering, in particular the so-called "polymerization peak" and amorphous "halo". In contrast to the united-atom model, the all-atom model was found to give a result that disagrees with the experiment. Structure, especially the X-ray structure factor of atactic PS, has been studied with MD simulation recently by Ayyagari, Bedrov, and Smith.[12] It was found that the amorphous peak in atactic PS arises mainly because of phenyl−phenyl correlations and that intra- and intermolecular interactions play an important role.

In contrast to the studies of its structural properties, data on the local dynamics of amorphous PS above and in the vicinity of T_g are scarce. One of the first MD simulations of bulk PS of different tacticity was performed by Tiller[14] for short chains of $N_p = 25$ monomers at $T = 300$ K and for quite short times up to 10 ps. Analysis of the dipole autocorrelation functions, for identifying the frequencies of the characteristic motions related to dielectric relaxation, reveals localized motions of the backbone segments and librational motions of the pendant phenyl groups. Han, Gee, and Boyd[15] performed MD simulations of different amorphous polymers (*cis*-poly(1,3-butadiene), polyisobutylene, atactic polypropylene, and polystyrene). They showed that the values from the MD-determined volume−temperature curves tend to be displaced to somewhat higher temperatures compared to typical experimental values. Nevertheless, the displacements are minor compared to the range of T_g values considered (almost 200 K). A similar conclusion was drawn from the MD simulations of atactic polypropylene,[6] poly(vinyl chloride),[16] bisphenol A polycarbonate,[17] and polyethylene.[18−23]

Local orientational mobility in bulk amorphous PS has been investigated by Khare and Paulaitis[24] through the study of cooperative phenyl ring flip motions near T_g with the help of transition-state theory. The main conclusion of ref 24 is that the local intrachain steric interactions, which dominate rotation in single chains, do so in the polymer glass as well. Local translational mobility of a single PS chain of $N_p = 80$ monomer units has been investigated by MD simulations of Roe[25] in the time range up to 600 ps and in the vicinity of T_g, but only at atmospheric pressure. Two distinct regimes in the local translational dynamics have been established: (i) diffusive motion at times less than 1 ps and (ii) at larger times a relatively slower dynamics, which is nearly frozen at or below the glass-transition temperature.

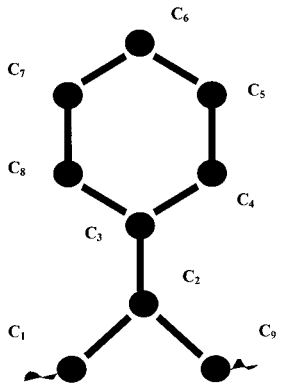

Figure 1. United-atom model of atactic polystyrene with numbered atoms in the monomer unit.

The present paper mainly serves as a base for our future study of the local segmental dynamics (translational and rotational), both in the isotropic state and under the influence of anisotropic uniaxial deformation, of amorphous polymers, such as PS, polycarbonate, and poly(methyl methacrylate). In this paper we intend to investigate some localized translational motions in glassy PS in much more detail than before, exploring for the first time a rather broad pressure−temperature range. The possibilities of MD simulations for reproducing the existing experimental PVT data at different pressures, and the glass-transition temperature at pressures higher than existing experimental data, are also investigated.

In short, we perform here computer simulations for the united-atom model of bulk atactic PS similar to[13,25] but (i) for much longer chains (up to 320 monomer units), and in rather broad temperature range; (ii) with an eye on possible molecular weight dependencies, in particular for the cage release time and the onset of the diffusive regime in the vicinity of T_g; (iii) in a broader pressure range (up to 1000 MPa); and (iv) for larger time scales (up to few tens of nanoseconds). To do so, a well-optimized molecular-dynamics simulation code based on the program GBMOL[26] has been used.

The present paper addresses these issues by employing constant-pressure (for the equilibration) and constant-energy (for the production) molecular dynamics techniques. The model, algorithm, and other details of the simulation, especially the equilibration procedure, are presented in section 2. Our results on the glass-transition temperature and the local translational mobility are discussed in section 3, and the main conclusions are summarized in section 4.

2. Model and Details of the Simulation

According to Mondello et al.,[13] his all-atom model for PS produces results that agree less well with the experiment than the united-atom model. Following this conclusion and to save the computational time, we have chosen the united atom model of PS also in the present paper. The model consists of a single polymer chain of $N_p = 40-320$ monomers (molecular weight from ∼4000 to ∼33 000) and its periodic images generated by periodic boundary conditions. The monomer unit (9 united atoms) of the model is shown in Figure 1.

The stereochemic configurations of the aromatic groups were generated at random so that the ratio of number of meso to number of racemic dyads was near

unity. The interaction potential has the following general form

$$U = \sum_{|i-j|\le 3} \epsilon[(r_0/r_{ij})^{12} - 2(r_0/r_{ij})^6] + \sum_k k_\theta(\theta_k - \theta_0)^2 + \sum_l k_\varphi(1 - \cos 3\varphi_l) + \sum_m k_\chi \cos^2(\chi_m - \chi_0) + \sum_n k_\psi {\psi_n}^2 + \sum_{k_{arom}} \hat{k}_\theta(\theta_{k_{arom}} - \hat{\theta}_0)^2 + \sum_{i_{arom}} \hat{k}_\varphi(1 + \cos 2\varphi_{i_{arom}}) + U_{imp}$$

The following contributions to U have been considered: (i) nonbonded interactions ($\sim\epsilon$) between all united atoms three or more bonds apart; (ii) bending potential ($\sim k_\theta$, $\hat{k}_\theta$) for all bond angles including those in the phenyl rings; (iii) torsional potential ($\sim k_\varphi$) for the backbone; (iv) torsional potential ($\sim k_\chi$) for the phenyl ring torsions; (v) phenyl ring ($\sim k_\iota$) out-of-plane bending potential; (vi) torsional potential ($\sim \hat{k}_\varphi$) about $-C_{arom}-C_{arom}-$ bond; (vii) improper torsion potential, U_{imp}.

All potential contributions and potential constants are identical to ref 13 except the last three terms. Instead of keeping the planarity of the aromatic rings by imposing some geometrical constraints as has been done in ref 13, we implement a bond-bending potential for all valence angles in the phenyl rings, with spring constant $\hat{k}_\theta = 301$ kJ/mol and $\hat{\theta}_0 = 120°$. In addition, a 2-fold rotational potential in the form proposed by Han and Boyd[27] with the value of $\hat{k}_\varphi = 54$ kJ/mol has been used for the rotations around the $-C_{arom}-C_{arom}-$ bond. Finally, to prevent the collapse of the four united atoms, C_2, C_4 and C_3, C_8 onto a plane, an improper torsion potential in the form proposed in ref 28 has been used:

$$U_{imp} = (1/6k')(\Delta_{129} + \Delta_{123} + \Delta_{329})^6 \qquad (2)$$

where $\Delta_{ijk} = \cos\theta_{ijk} - \cos\theta_0$ with $\theta_0 = 109.5°$ and θ_{ijk} is the bending angle formed by the C_i, C_j, and C_k united atoms according to the numbering of Figure 1. This contribution to the force field, with $k' = 150k_\theta = 37\,355$ kJ/mol, does not affect small-amplitude vibrations but has been added in an ad hoc way to prevent the onset of accidentally large-amplitude fluctuations which could lead to the occurrence of a planar conformation of the three bonds attached to the C_2 united atom.

For numerical expediency the term with bond stretching contribution is excluded from the interaction potential. The length of all valence bonds has been constrained by the SHAKE iterative procedure[29] with the relative tolerance of 10^{-6}. In SHAKE the total force acting on a bead is expressed as the sum of the force deriving from the potential energy U and the forces of constraint which act along the rigid bonds. Lagrange multipliers associated with these constrained forces are calculated iteratively.

The leapfrog variant of the velocity Verlet algorithm[30] has been used to integrate the Newtonian equations of motion. Much attention was paid to the equilibration of the system. Equilibration has been performed by the Berendsen NPT molecular dynamics algorithm,[31] with time constants $\tau_T = 0.5$ ps and $\tau_P = 1$ ps and with an integration time step $\Delta t = 4$ fs. At the very beginning the all-trans conformation of an atactic PS chain was generated and immersed into the simulation box of rather big size (about 300 Å) in order to avoid possible close contacts of nonbonded united atoms. The box was allowed to relax under the fixed imposed external pressure (usually 1−10 MPa) and at a rather high initial temperature ($T = 600$ K) for sufficiently long time (10−20 ns, depending on the chain length) until the final equilibrium structure was produced. The global equilibration of the system was controlled by measuring different conformational properties such as the end-to-end distance and radius of gyration of the chain. The density of the polymer melt was also calculated. At $T = 560$ K for the chain of $N_p = 80$ monomers the pressure was adjusted in order to reproduce the experimental density of 910 kg/m^3 for PS of approximately the same molecular weight.[32] This value of pressure correction was used for all lower temperatures. The equilibration of the intermediate scales has been checked as well by measuring the distances between different inner parts of the chain (beads separated by N_m bonds, where $N_m = 5$, 10, and 20). To control the quality of such an equilibration, different initial conformations of the chain have been used also. In particular, the random coil has been generated by a Monte Carlo procedure with the possibility to avoid rather close contacts of nonbonded united atoms (when the distance between any possible pair of beads is smaller than $0.8r_0$, r_0 being the characteristic length parameter of the excluded-volume interactions). Some runs have been performed using initial structures generated by the MSI Materials Studio Amorphous Cell interface. The calculated final conformational properties and final density were identical to those produced earlier from the all-trans initial conformation.

After such a compression the external pressure was fixed to the desired value and equilibration continued for another 5−10 ns depending on the chain length. All equilibrium structures for lower temperatures were produced by cooling the system down with a temperature step of 20 K. For the largest systems studied here ($N_p = 320$ monomers, 2561 united atoms) the total duration of the equilibration for a single pair of temperature and pressure values was about 30 ns. The equilibrium conformation of a single chain of $N_p = 80$ monomers at atmospheric pressure and temperature $T = 540$ K is shown in Figure 2.

After the equilibration procedure described above, the production runs have been performed by NVE MD with the integration step of $\Delta t = 2-2.5$ fs. In all cases the length of these runs was from 10 to 30 ns. During these microcanonical runs the ratio of the mean-square fluctuations of kinetic energy to those of the total energy was always in the limit of 3−4%. No drift in the total energy was observed. On a single-processor Origin 2000 computer an integration time step took about 0.02 s for a chain of $N_p = 80$ monomers.

3. Results and Discussion

A. Determination of the Glass Transition Temperature. The last 1−3 ns of the trajectories produced by NPT runs was used to determine the specific volume. The standard mean-square dispersion of the data was used to estimate the statistical errors. The temperature dependence of the specific volume at different values of pressure is shown in Figure 3a for the model with $N_p = 80$ monomers. The specific volume decreases almost linearly at both high and low temperature with decreasing temperature. At atmospheric pressure the clear change in the thermal expansion coefficient occurs at $T_g \sim 370$ K and serves as an indication of the glass transition. The dashed lines in Figure 3a represent the experimental data of standard pressure−volume−tem-

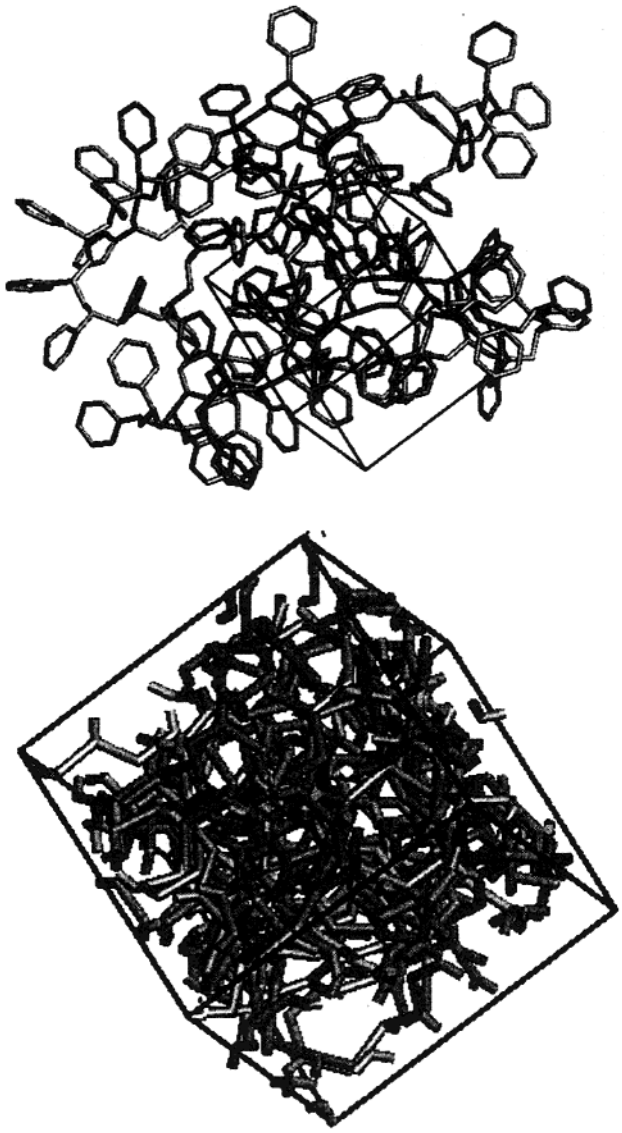

Figure 2. (a, top) Snapshot of the equilibrated conformation ($T = 540$ K, $P = 0.1$ MPa) of the single PS chain with $N_p = 80$ monomers. The simulation box of length $L \sim 24$ Å is also shown. (b, bottom) The same conformation but with periodic boundary conditions.

perature measurements for atactic polystyrene of $M \sim 9000$,[32] which is close to the molecular weight of the 80-monomer model studied here. The agreement is quite satisfactory despite the obvious difference in the cooling rates—a few deg/s in the experiment as compared to 20–50 K/ns in the MD simulations.

At different values of pressure the curves were fitted by two straight lines using the least-squares fit. Data above and below the published value of T_g were used to produce high-temperature and low-temperature fits. The intersection of these two lines is used to determine the glass-transition temperature. Simulations from two independent initial configurations obtained from the MSI Amorphous Cell interface have been also performed in order to check the reproducibility of the data. The error bars in Figure 3 are produced by averaging the results from different simulation runs. A similar procedure of determining T_g was used recently by Fried and Li[33] in molecular dynamics simulation of disubstituted polysilanes.

At all values of pressure the MD-determined T_g is higher than the corresponding experimental value from

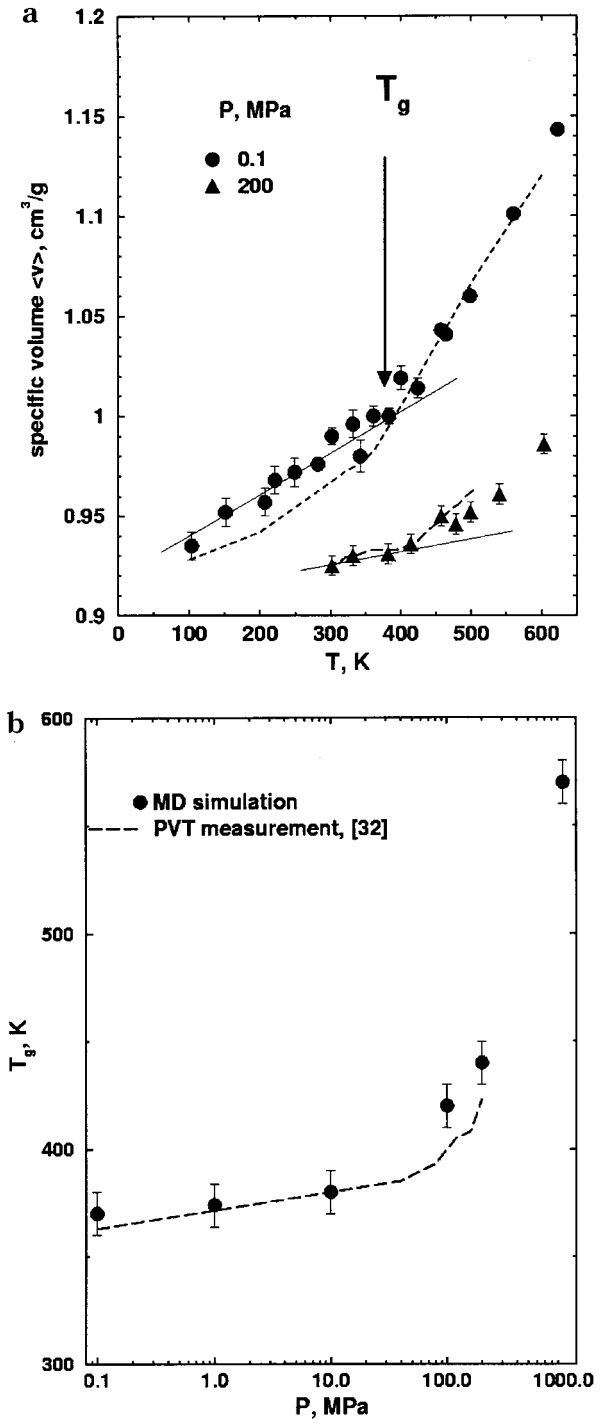

Figure 3. (a) Temperature dependence of the specific volume obtained in the simulations at $P = 0.1$ MPa (circles) and $P = 200$ MPa (triangles) for the $N_p = 80$ monomers PS chain. Dashed lines represent the experimental data for the atactic polystyrene of $M \sim 9000$ at corresponding pressures.[32] The arrow indicates the simulated value of T_g (370 K) at atmospheric pressure $P = 0.1$ MPa. Solid lines represent the least-squares fit of data at low temperature. (b) Pressure dependence of the MD-determined T_g (circles) for the $N_p = 80$ monomers chain. The dashed line represents the experimental data for the atactic polystyrene of $M \sim 9000$.[32] Error bars indicate the statistical errors of least-squares parameters used to fit the data in (a).

ref 32, but the difference is only a few degrees. Increasing the PS molecular weight from 4000 (degree of polymerization $N_p = 40$) to 33 000 ($N_p = 320$) shifts the value of T_g from 370 to ~375 K at atmospheric pressure. Existing experimental data[32] show a shift from ~360

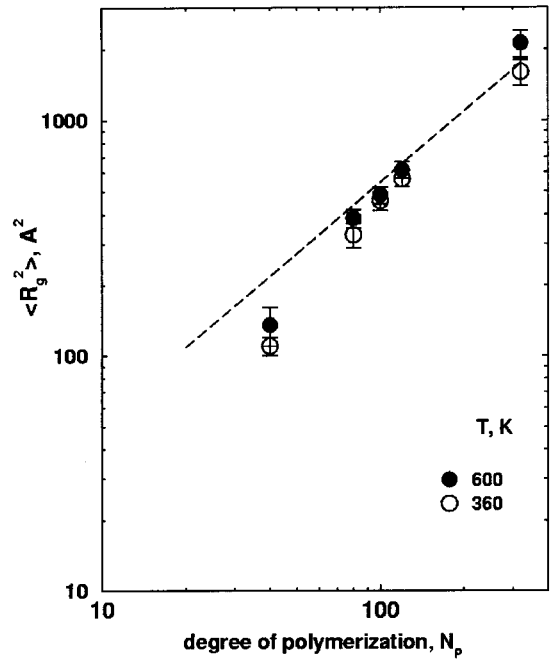

Figure 4. Dependence of the mean-square radius of gyration $\langle R_g^2 \rangle$ on degree of polymerization N_p at different temperature: $T = 600$ K (closed symbols) and $T = 360$ K (open symbols). The dashed line gives a slope equal to 1. Error bars were estimated from the dispersion of the data obtained from the simulations started from independent initial configurations.

to 365 K when increasing the molecular weight from 9000 to 110 000.

Increasing the external pressure leads to some increase of the glass-transition temperature (Figure 3b). The MD data suggest that the value of T_g increases by 70 K from ~370 to ~440 K when the pressure increases from 0.1 to 200 MPa. Experimental data[32] give a shift from ~360 to ~420 K. At the same values of the external pressure a slightly smaller increase in the value of T_g, from 300 to 350 K, was observed in ref 23 by MD simulation of a model PE system.

MD results show that T_g increases dramatically with increasing pressure from 200 to 1000 MPa (Figure 3b). Unfortunately, no experimental data at these pressures are available for comparison.

B. Radius of Gyration. At high temperature, $T > T_g$, and in the glassy state ($T = 360$ K) the mean-square radius of gyration increases almost linearly with increasing molecular weight, confirming the applicability of the Rouse model to the polymer melt (Figure 4). Two different initial configurations (produced by equilibration runs started from all-trans and coiled conformations, as explained in section 2) have been used. For 40-mers and 80-mers melts two additional initial configurations obtained from the simulations with the MSI Amorphous Cell interface have been also used for final averaging. The mean value of R_g in the glassy state is a bit smaller than in the melt, but at the same time the error bars are rather high. For the chain of $N_p = 80$ monomers, $M \sim 8300$, the radius of gyration is $R_g = 19.6 \pm 1$ Å at $T = 600$ K and atmospheric pressure (0.1 MPa), to be compared with the expected value of 22.3 Å (±15%) from Rapold et al.,[11] who used the experimental value of the characteristic ratio $C_\infty = \langle r^2 \rangle / N_p l^2 = 9.2$ (here r is the end-to-end distance and l is the main chain bond length) in their Monte Carlo simulations. Results of Mondello et al.[13] give the average value of

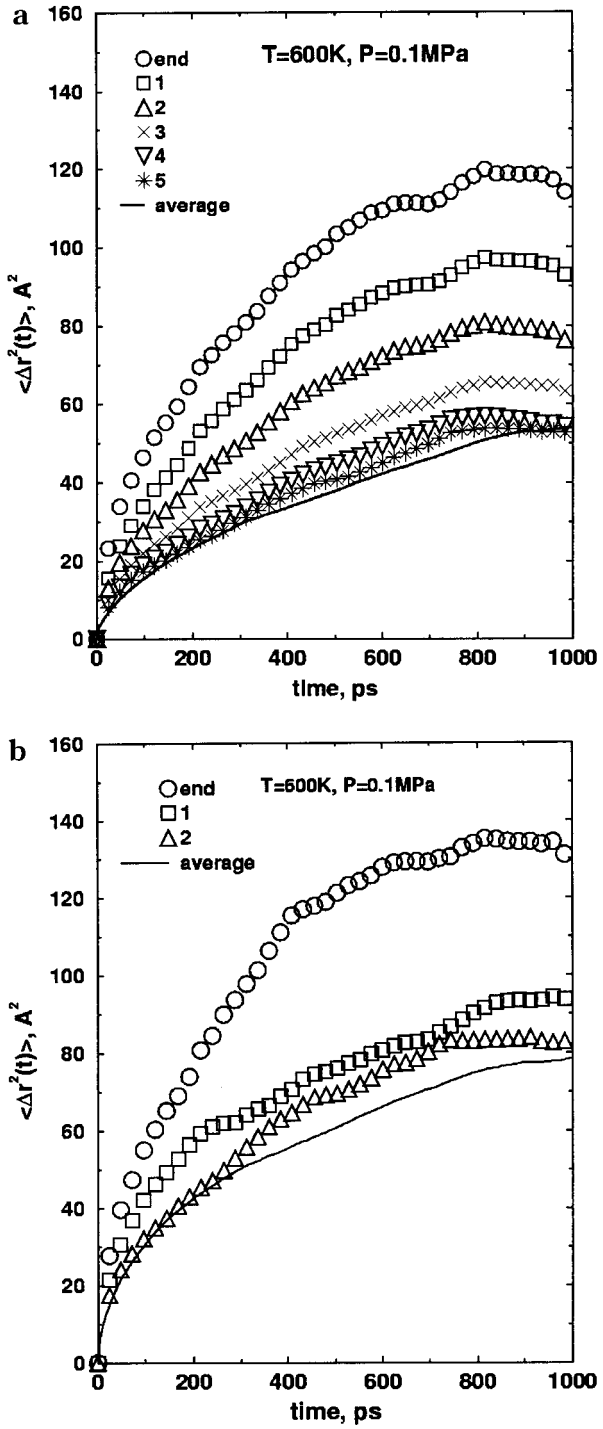

Figure 5. (a) Mean-square translational displacements of beads in the main chain at $T = 600$ K and $P = 0.1$ MPa (melt), $N_p = 80$ monomers chain. Beads at the chain ends (circles) are the most mobile. Increasing the distance from the chain ends (numbers in the legend indicate the sequence number of the bead, starting from the end of the chain) leads to the pronounced decrease in translational mobility. Displacement of the average bead in the middle of the chain is shown by solid line. (b) The same as in (a) but for the beads in phenyl groups. The bead in the second phenyl group (numbering starts from the chain ends) has almost the same translational behavior as the bead in the average phenyl group in the middle of the chain.

$R_g = 25$ Å for $T = 540$ K and $P = 0.1$ MPa. This value of R_g was produced in ref 13 by averaging three values of the radius of gyration, 13.3, 14.7, and 38.4 Å, obtained from three independent runs of 500 ps each. Monte

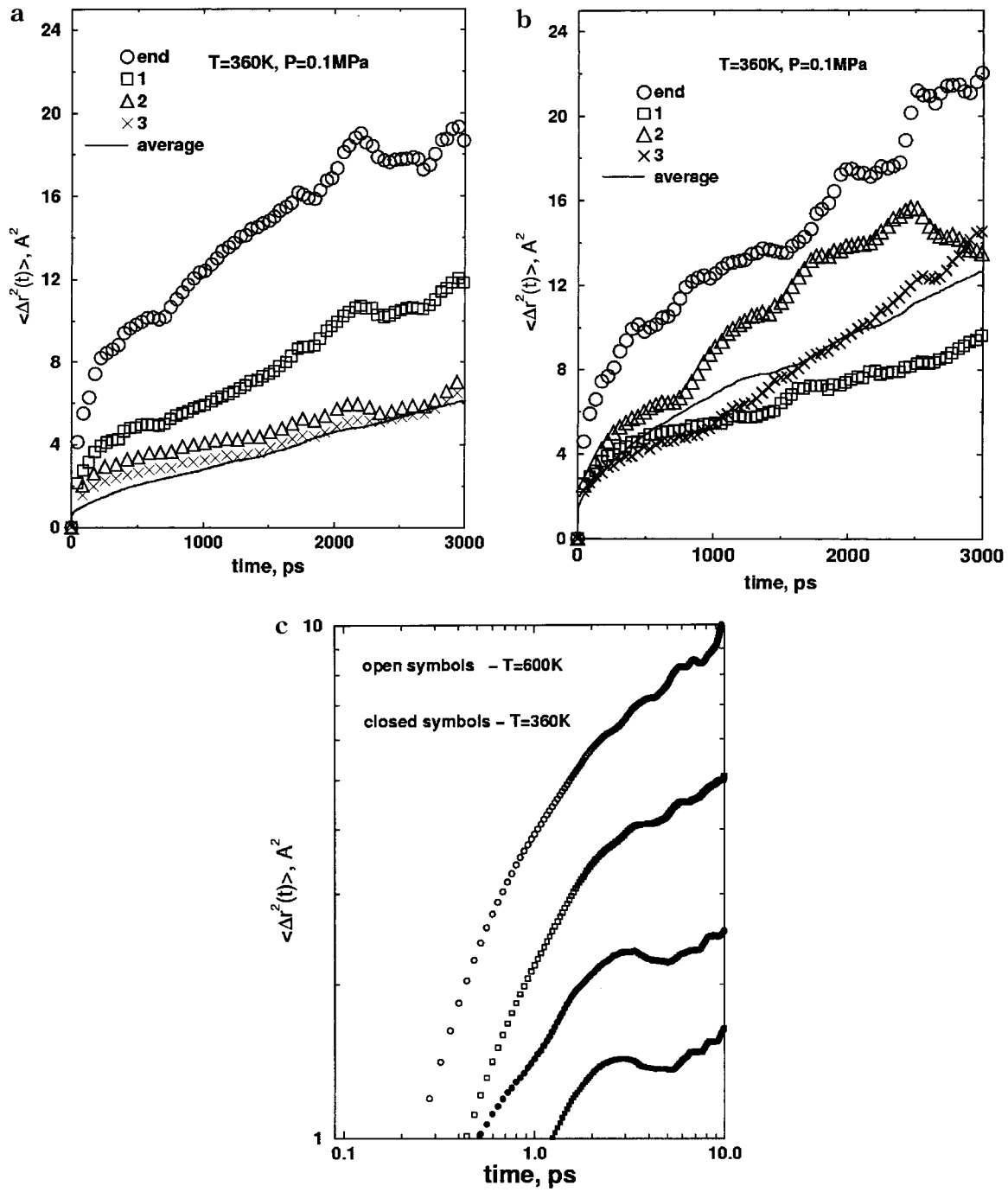

Figure 6. (a) Mean-square translational displacements of beads in the $N_p = 80$ monomers main chain at $T = 360$ K and $P = 0.1$ MPa (glassy state). End beads (circles) are the most mobile. Increasing the distance from the chain ends (numbers in the legend indicate the sequence number of the bead, starting from the end of the chain) leads to a pronounced decrease in translational mobility. Displacement of the average bead in the middle of the chain is shown by solid line. (b) The same as in (a) but for the beads in the phenyl group. The difference in mobility of different phenyl groups at this temperature is smaller than in the high-temperature case (Figure 5b). (c) Initial part (up to10 ps) of the mean-square displacements of the main chain end beads (circles) and the second from the end beads (squares) at two temperatures, $T = 600$ K (open symbols) and $T = 360$ K (closed symbols). Below T_g the momentary reversal of motion is seen in agreement with the results reported by Roe.[25]

Carlo simulations of Kotelyanskii et al.[34] give the values of $C_{64} = 6.3$ and $C_{364} = 7.3$ for the PS model with 64 and 364 monomers, respectively, in agreement with $C_{80} = 6.2$ result of the present simulation. Moreover, present MD results for the longest 320-mers PS chain give the value of $C_{320} \approx 8.5$ even closer to the experimentally observed values of C_∞.

Increasing the pressure to 100 MPa in the present simulations leads to about 10% decrease in the magnitude of the radius of gyration at each fixed temperature.

C. Local Translational Mobility: Influence of the Chain Ends. Local translational mobility has been studied by measuring the mean-square displacements $g(t)$, eq 1, of the beads both in the main chain and in the phenyl groups. (In the last case the averaging through all six beads in the aromatic ring has been performed.) At high temperature, $T = 600$ K, the mobility of the backbone groups is quite different from that of phenyl rings. Phenyl side groups are more mobile than the corresponding beads in the main chain: at

fixed time their mean-square translational displacements are larger than those of the main-chain monomers. This difference is not that dramatic for the terminal beads but is quite pronounced for the middle of the chain (the difference is about 50% in this case), because in the last case a noticeable displacement of the backbone bead requires rather big distortions of both chain tails attached to this bead. Translational displacements of the side groups do not require such big backbone perturbations.

In both cases the absolute value of the translational displacement at a fixed moment of time strongly depends on the distance from the chain ends. The terminal beads are about 3 times more mobile than the average bead in the middle of the chain. (The averaging was performed for all but the first 10 beads from each of the chain ends.) Figure 5 shows the results for the $N_p = 80$ chain at atmospheric pressure, but the same effect was observed for all other molecular weights and magnitudes of pressure studied here. As the distance from the ends increases, the mean-square translational displacements of the backbone beads are getting closer to that of the average bead in the middle of the chain. The fifth bead from the chain end is as mobile as the average bead. A qualitatively similar picture is valid for the side groups, but in this case the translational mobility of the second side-group bead from the chain ends is already close to that of the bead in the middle of the chain (Figure 5b).

The magnitude of the translational displacements decreases significantly when approaching the glass-transition temperature (Figure 6).

The "chain-ends" memory effects for the backbone beads are getting weaker when decreasing the temperature: the second bead from the chain end (either in the backbone or in the aromatic ring) moves similar to the average bead in the middle. Deep in the glassy state ($T < 200$ K) local translational mobility of all monomers is almost frozen.

D. Local Translational Mobility: Cage Effect. The mean-square displacements of the average bead both in the backbone and in the side group at different temperatures and atmospheric pressure are shown in Figure 7. For a free Brownian particle not included in the chain the Einstein formula is valid

$$\langle \Delta r^2(t) \rangle = 6Dt \qquad (3)$$

where $D = k_B T/\zeta$ is the particle translational diffusion coefficient and ζ is its translational friction coefficient. To remove the trivial temperature dependence, all curves in Figure 7 are normalized to the ratio T_0/T where $T_0 = 600$ K is some reference temperature.

At small times, $t < 1$ ps, these normalized dependencies do not depend on temperature (for both the main chain and side groups). In this case the slope for the main-chain monomers is 1.1 (in the log−log scale) in the whole temperature range studied here. For the phenyl rings the slope is 1.7, which is closer to 2 as would be the case for the pure ballistic regime.

In the high-temperature region, $T > T_g$, the asymptotic slopes of these dependencies (when time is much larger than 1 ps) are close to 0.6 (0.61 for the main chain and 0.54 for the side groups), in nice agreement with the results of refs 2 and 3. The difference from the prediction of the Rouse model, which gives the slope equal to 0.5, could be explained by the rather short length (even when $N_p = 320$) of the chain models under study here. The validity of the Rouse model for the description of the polymer dynamics in the melt could be also questionable, but the answer to this question requires simulations of much longer chains.

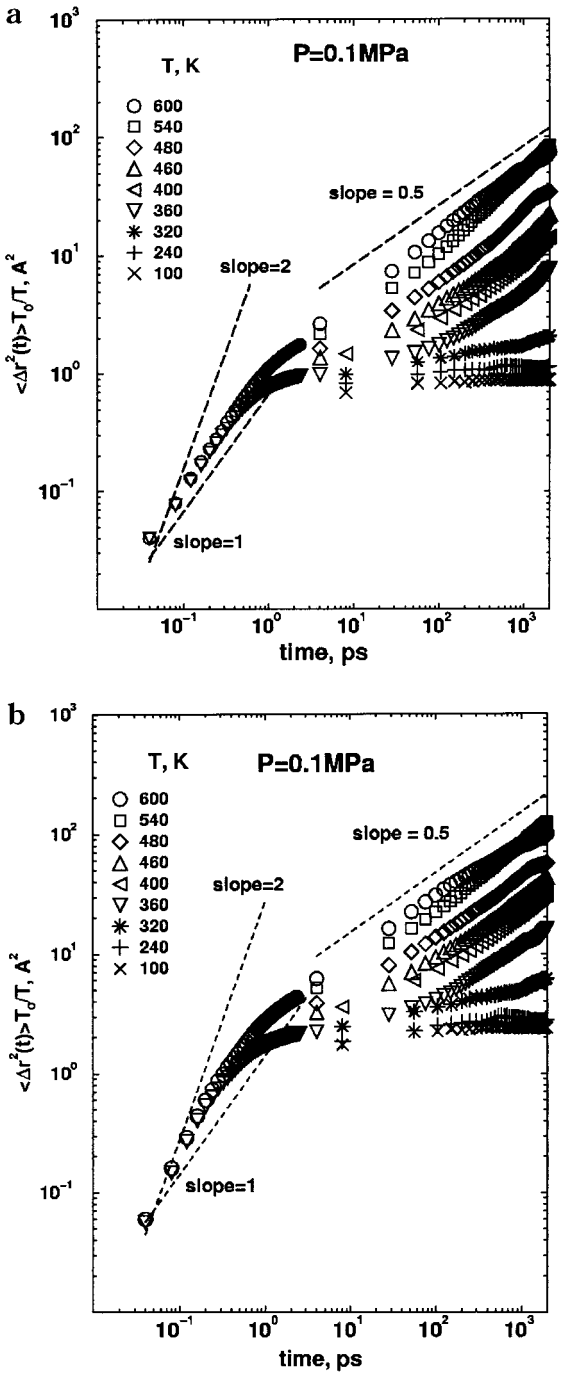

Figure 7. (a) Mean-square translational displacement of the average bead in the backbone of the $N_p = 80$ monomers chain at different temperatures. A diffusive regime with slope between 1 and 2 is observed for all temperatures up to $t = 1$ ps. An asymptotic slope of about 0.6 is confirmed for temperatures close to T_g and higher. Crossover between these two regimes is a manifestation of the cage effect when the motion of chain monomers is restricted to some cage formed by the almost frozen neighborhood. (b) The same as in (a) but for the average bead in the average phenyl group in the middle of the chain. The cage effect is also clearly seen at $T < T_g$.

In the vicinity of T_g two regimes of translational mobility—the first with the slope between 1 and 2 and the second with the slope of ~0.6—are separated by some plateau. The size of this plateau increases with

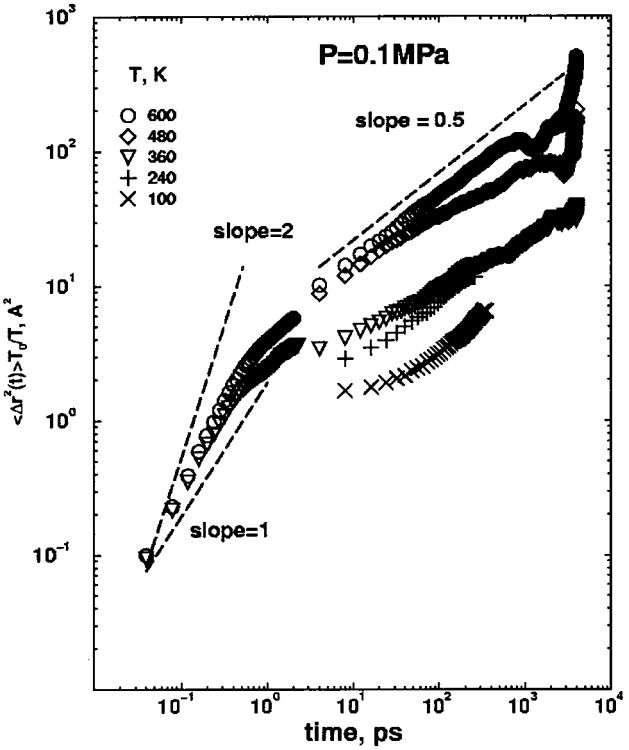

Figure 8. Mean-square translational displacement of the end bead of the $N_p = 80$ monomers PS main chain at different temperatures. The cage effect is not that pronounced as for the average bead in the middle of the chain (Figure 7); even at rather low temperature (100 K) the onset of the diffusive regime with the slope ~0.6 is established.

decreasing temperature. At low temperatures, $T < 240$ K, translational mobility is almost frozen, and the plateau continues until the maximum times available in the present simulations (about 30 ns). This picture is qualitatively the same for all values of pressure (up to 1000 MPa) used in this paper.

Crossover between the two regimes of the translational diffusion is known as the cage effect:[5,25] very restricted local motions occur in the cage formed by surrounding monomers. In ref 25 it is demonstrated that the cage effect can be displayed by momentary reversal of motion. This effect is seen in Figure 6c where such a reversal in the mean-square displacement of the main chain segments at $T = 360$ K occurs at about 2 ps. For a pure ballistic motion of the bead inside the cage, $\langle \Delta r^2(t) \rangle = v^2 t^2$ where v is the average thermal velocity, easily estimated from the equipartition theorem (taking into account only translational motions for simplicity) at $T = 360$ K as ~830 m/s. The size of that cage can be estimated from the onset of the plateau regime, $\langle R_{cage}^2 \rangle^{1/2}$. The ratio $t_{ball} = \langle R_{cage}^2 \rangle^{1/2}/v$ can serve as the characteristic "ballistic" time of the bead motion inside the cage. Estimations give $t_{ball} = 0.09$ ps for the backbone bead and $t_{ball} = 0.21$ ps for the bead in the phenyl ring.

The plateau regime starts when $t > t_{cage} \sim 2.5$ ps both for the main chain bonds and side groups. This time is at least the order of magnitude larger than that of the ballistic motion. The time of the free inertial motion of the phenyl ring bead is more than 2 times larger than that for the bead in the backbone, and the onset of the diffusive regime with $\langle \Delta r^2(t) \rangle \sim t$ is starting later. The fact that for the phenyl rings the initial slope (1.7) is larger than for the main chain beads is also a sequence of "more ballistic" motion of side groups inside a cage.

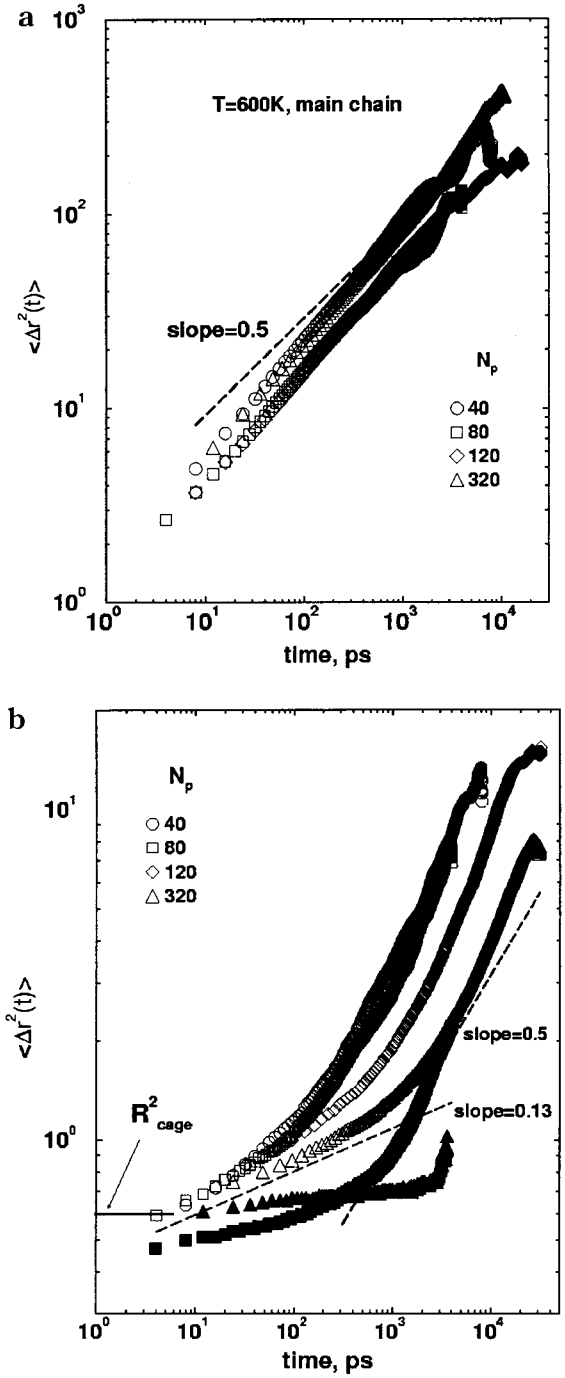

Figure 9. (a) Mean-square translational displacement of the average bead in the backbone of the chains with different degree of polymerization (from $N_p = 40$ to $N_p = 320$ monomer units) at $T = 600$ K and $P = 0.1$ MPa. All curves show the asymptotic slope close to 0.6 and are very close to each other in the studied region of times (up to 10 ns). (b) Mean-square translational displacement of the average bead in the backbone of the chains with different degree of polymerization (from $N_p = 40$ to $N_p = 320$ monomer units) at $T = 360$ K (close to T_g), open symbols, and $T = 350$ K, closed symbols, at atmospheric pressure, $P = 0.1$ MPa. The size of the cage at $T = 360$ K is indicated by solid line. The asymptotic regime with the slope of about 0.6 is starting at larger times with increasing the molecular weight or decreasing the temperature.

The cage effect is not very pronounced for the more mobile backbone ends (Figure 8). At $T = 360$ K (close to, but still below, T_g) the first regime, with the slope of ~1.3, is immediately followed by the diffusion with the slope very close to 0.5. Even at very low temperature,

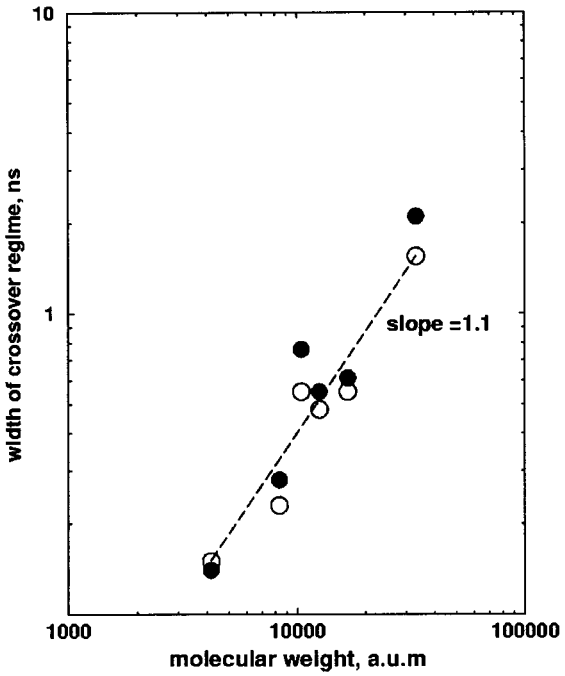

Figure 10. Molecular weight dependence of the characteristic time of the onset of the second diffusive regime for the backbone monomers (closed circles) and phenyl groups (open circles) at $T = 360$ K. Dashed line shows a power law fit which gives a slope very close to unity.

$T \sim 100$ K, the onset of this diffusion starts at times $t \sim 0.1$ ns.

High-temperature and low-temperature mean-square translational dependencies are shown in Figure 9 for chains of different degree of polymerization, from $N_p = 40$ to $N_p = 320$ monomers, at atmospheric pressure.

In the melt ($T > T_g$) the asymptotic slope for all curves is very close to 0.6. All curves are rather close to each other; no regular molecular weight dependence is observed. However, increasing the molecular weight leads to a broadening of the crossover regime. The onset of the diffusion with the slope about 0.6 starts at larger times for the chains with larger degree of polymerization. It should be noticed that the onset of the developed asymptotic regime starts, from the computational point of view, at very large times (above 1 ns) which makes all simulations rather expensive. At $T < T_g$ these curves are very close to each other for different molecular weights but only up to the time $t \sim 100$ ps. The initial slope of the curves in Figure 9b does not depend on molecular weight either and is very close to 0.13. This time, $t \sim 100$ ps, could serve as the characteristic cage release time. It is clear that the onset of the diffusive regime starts later for rather long chains with $N_p > 100$. Decreasing the temperature from $T = 360$ K to $T = 350$ K also leads to the pronounced broadening of the crossover area (Figure 9b).

One can try to extract the characteristic time of onset of the well-developed diffusive regime by fitting the *final* parts of the curves in Figure 9b with the power law, $\langle \Delta r^2(t) \rangle \sim t^{\alpha}$, and looking for the time at which the original curves start to decline significantly from the fits. Of course this procedure can give only rather crude approximation to the possible, if any, molecular weight dependence of this time. In Figure 10 the molecular weight dependence of these times is fitted to a power law, giving a slope very close to unity.

It should be noted that the slope of the order of unity in Figure 10 is produced by both backbone beads and the beads in the phenyl rings. For long chains ($N_p > 100$) the possible entanglements could play a role when studying the local translational mobility, and the intermediate diffusive regime should be investigated. A detailed and much more precise investigation of the possible molecular weight dependence of the crossover from the cage release to well-developed diffusive motion requires the simulation of much longer chains in sufficiently large intervals of times.

4. Conclusions

We have performed molecular dynamics simulations of the united atom model of bulk atactic polystyrene, both in the melt and in the glassy state, considering a much larger parameter space (time, pressure, temperature, molecular weight) than previously reported.[13,25] It was shown earlier[13] that this model reproduces well the main peculiarities of the glass transition at atmospheric pressure. The range of the values of pressure studied in the present paper was extended to 1000 MPa. The MD determined value of T_g shifts from 370 to 440 K when pressure changes from 0.1 to 200 MPa. This shift is in perfect agreement with the existing experimental data. Increasing the pressure from 200 to 1000 MPa leads to dramatic increase in the value of T_g. It would be very desirable to compare these results with experimental data. We did not perform a detailed study of the molecular weight dependence of T_g, but the first preliminary results show that increasing the molecular weight does not change the location of the glass transition significantly.

In this paper the main attention was paid to the investigation of the local translational mobility of both the monomers in the main chain and in the phenyl side groups. The mobility of the chain ends influences the translational mobility of only a few neighboring monomers (3−5 nearest neighbors), both in the backbone and in the aromatic side groups. The average monomer in the middle of the model PS chain, even with $N_p = 40$ monomers, can already serve as a representative monomer for the high molecular weight PS.

In the vicinity of the glass-transition temperature two diffusive regimes of the local translational mobility are clearly separated by a crossover regime describing the motions confined in cages formed by almost frozen neighborhood. The first regime of the translational mobility takes place at rather short times, $t \sim 1$ ps, and is an intermediate one between ballistic motion, with $\langle \Delta r^2(t) \rangle \sim t^2$, and free-monomer diffusive motion, with $\langle \Delta r^2(t) \rangle \sim t$. The second diffusion regime, with $\langle \Delta r^2(t) \rangle \sim t^{\alpha}$ and $\alpha \sim 0.6$, characterizes the local diffusion of monomers inside the polymer chain. The width of the crossover increases with increasing molecular weight. Our results show almost linear molecular weight dependence for the width of the crossover regime, but detailed simulations of much longer chains are necessary to make definite conclusions.

Acknowledgment. This work is the part of the research program of the Dutch Polymer Institute. Grateful acknowledgment is made to U. Suter (ETH Zürich), J. P. Ryckaert (ULB, Belgium), P. v. d. Schoot (TUE, The Netherlands), H. Slot, and A. Stroeks (DSM Research, The Netherlands) for many useful discussions.

References and Notes

(1) Binder, K.; Baschnagel, J.; Böhmer, S.; Paul, W. *Philos. Mag. B* **1998**, *77*, 591.
(2) Binder, K.; Baschnagel, J.; Bennemann, C.; Paul, W. *J. Phys.: Condens. Matter* **1999**, *11*, A47.
(3) Bennemann, C.; Paul, W.; Binder, K.; Dünweg, B. *Phys. Rev. E* **1998**, *57*, 843.
(4) Kremer, K.; Grest, G. S. *J. Chem. Phys.* **1990**, *92*, 5057.
(5) Bennemann, C.; Baschnagel, J.; Paul, W.; Binder, K. *Comput. Theor. Polym. Sci.* **1999**, *9*, 217.
(6) Yip, S.; Sylvester, M. F.; Argon, A. S. *Comput. Theor. Polym. Sci.* **2000**, *10*, 235.
(7) van Zon, A.; de Leeuw, S. W. *Phys. Rev. E* **1999**, *60*, 6942.
(8) See Götze, W. In *Liquids, Freezing and the Glass Transition*; Hansen, J. P., Levesque, D., Zinn-Justin, J., Eds.; North-Holland: Amsterdam, 1991.
(9) Baschnagel, J. *Phys. Rev. E* **1994**, *B49*, 135.
(10) Leutheusser, E. *Phys. Rev. A* **1994**, *A29*, 2765.
(11) Rapold, R. F.; Suter, U. W.; Theodorou, D. N. *Macromol. Theory Simul.* **1994**, *3*, 19.
(12) Ayyagari, C.; Bedrov, D.; Smith, G. *Macromolecules* **2000**, *33*, 6194.
(13) Mondello, M.; et al. *Macromolecules* **1994**, *27*, 3566. Furuya, H.; et al. *Macromolecules* **1994**, *27*, 5674. Roe, R. J.; et al. *Macromolecules* **1995**, *28*, 2807.
(14) Tiller, A. R. *Macromolecules* **1992**, *25*, 4605.
(15) Han, J.; Gee, R. H.; Boyd, R. H. *Macromolecules* **1994**, *27*, 7781.
(16) Abu-Sharkh, B. F. *Comput. Theor. Polym. Sci.* **2001**, *11*, 29.
(17) Fan, C.; Çagin, T.; Shi, W.; Smith, K. A *Macromol. Theory Simul.* **1997**, *6*, 83.
(18) Roe, R. J. *J. Chem. Phys.* **1994**, *100*, 1610.
(19) Boyd, R. H.; Gee, R. H.; Han, J.; Jin, Y. *J. Chem. Phys.* **1994**, *101*, 788.
(20) Jin, Y.; Boyd, R. H. *J. Chem. Phys.* **1998**, *108*, 9912.
(21) Gee, R. H.; Boyd, R. H. *Comput. Theor. Polym. Sci.* **1998**, *8*, 93.
(22) Bharadwaj, R. K.; Boyd, R. H. *Macromolecules* **2000**, *33*, 5897.
(23) Yang, L.; Srolovitz, D. J.; Yee A. *J. Chem. Phys.* **1999**, *110*, 7058.
(24) Khare, R.; Paulaitis, M. *Macromolecules* **1995**, *28*, 4495.
(25) Roe, R. J. *J. Non-Cryst. Solids* **1998**, *235−237*, 308.
(26) Lyulin, A. V.; Al-Barwani, M. S.; Allen, M. P.; Wilson, M. R.; Neelov, I. M.; Allsopp, N. K. *Macromolecules* **1998**, *31*, 4626.
(27) Han, J.; Boyd, R. H. *Polymer* **1996**, *37*, 1797.
(28) Destrée, M.; Lauprêtre, F.; Lyulin, A.; Ryckaert, J.-P. *J. Chem. Phys.* **2000**, *112*, 9632.
(29) Ciccotti, G.; Ferrario, M.; Ryckaert, J.-P. *Mol. Phys.* **1982**, *47*, 1253.
(30) Allen, M. P.; Tildesley, D. J. *Computer Simulation of Liquids*, Clarendon Press: Oxford, 1987.
(31) Berendsen, H. J. C.; Postma, J. P. M.; van Gunsteren, W. F.; DiNola, A.; Haak, J. R. *J. Chem. Phys.* **1984**, *81*, 3684.
(32) Zoller, P.; Walsh, D. J. *Standard Pressure−Volume−Temperature Data for Polymers*; Technomic: Lancaster, 1995.
(33) Fried, J. R.; Li, B. *Comput. Theor. Polym. Sci.* **2001**, *11*, 273.
(34) Kotelyanskii, M.; Wagner, N. J.; Paulaitis, M. E. *Macromolecules* **1996**, *29*, 8497.

MA011318U